

Journal of Materials Chemistry C

Accepted Manuscript



This is an *Accepted Manuscript*, which has been through the Royal Society of Chemistry peer review process and has been accepted for publication.

Accepted Manuscripts are published online shortly after acceptance, before technical editing, formatting and proof reading. Using this free service, authors can make their results available to the community, in citable form, before we publish the edited article. We will replace this *Accepted Manuscript* with the edited and formatted *Advance Article* as soon as it is available.

You can find more information about *Accepted Manuscripts* in the [Information for Authors](#).

Please note that technical editing may introduce minor changes to the text and/or graphics, which may alter content. The journal's standard [Terms & Conditions](#) and the [Ethical guidelines](#) still apply. In no event shall the Royal Society of Chemistry be held responsible for any errors or omissions in this *Accepted Manuscript* or any consequences arising from the use of any information it contains.



Journal Name

ARTICLE

Tunable Stokes Shift and Circular Polarized Luminescence by Supramolecular Gel

Received 00th January 20xx,
Accepted 00th January 20xx

DOI: 10.1039/x0xx00000x

www.rsc.org/

Hirokuni Jintoku,^a Min-Tzu Kao,^b André Del Guerzo,^b Yudai Yoshigashima,^a Takuya Masunaga,^a Makoto Takafuji^{a,c} and Hiroataka Ihara^{a,c*}

A new optical material based on the self-assembly of a low-molecular organogelator-linked anthracene derivative for the control of the fluorescence wavelength and polarization was developed. When the anthracene derivative was formed through self-assembly, the fluorescence wavelength was shifted by 100 nm (426 to 526 nm) and emitted circularly polarized luminescence. The control of the fluorescence wavelength and polarization was accomplished through the excimer formation of anthracene fluorophores, which can be tuned by the cooling process, temperature and solvent of the solution. Also, the fluorescence control in the solid state and the white-light emission in the gel state were accomplished by mixing the polymer matrix, and the addition of red-emitting dye, respectively. This material has possible potential for various applications such as a spectral conversion film, white light-emitting diodes and for circular polarized displays.

Introduction

Fluorescent materials have attracted a large amount of attention for applications such as in organic light-emitting diodes (OLEDs), solar cells, displays, and sensors.¹ The optical properties required for applications in these fields are a high fluorescence quantum yield and a controllable wavelength of fluorescence.² In particular, precise control of the emission wavelength, wide range-emission and multi-wavelength emissions may generate applications in a wide range of fields such as spectral conversion, white light emitting diode and for biomarkers.³ To accomplish this, two methods have been developed and proven to be successful. One of these is a synthetic approach,⁴ in which the fluorescence wavelength of a heterocyclic molecule and a π -conjugated polymer can be controlled by changing the chemical structure and conjugation length or by substitution of a side chain.⁵ These materials have the advantages of stability and precise control of the wavelength. However, multi-wavelength emission is accomplished only in special conditions such as excited-state intramolecular proton transfer and intramolecular charge-transfer.⁶ The other approach is through self-assembly, in which, for example, the fluorescence of low molecular weight organic molecules can be controlled by changing the molecular

orientation of the fluorophore.⁷ The fluorophore may respond to stimuli such as temperature, pH, light and pressure, reversing the fluorescence change.⁸

The self-assembly approach has great possibility for fabrication of unique fluorescent materials. However, there are some problems (for example, the stability and accuracy of the wavelength control) in practical use. To solve these problems, we exploited the properties of self-assembly of an L-glutamic acid derived lipid (**g**), which is a low molecular weight organic molecule.⁹ The molecule, **g**, can form various molecular orientation states with slight adjustments to its surrounding environment such as the solvent, temperature or additives.¹⁰ This is because of the sterically arranged amide bonds around the chiral carbon atoms. Also, the stability of the **g**-assembly can be enhanced by mixing it with the polymer matrix.¹¹ On the basis of these results, we present new compounds for the fabrication of a fluorescent material with a high quantum yield and controllable fluorescent wavelength. Anthracene derivatives were prepared for this study to act as the fluorescent unit. Anthracene is a good candidate for a fluorophore because of its high quantum yield and its ability to form excimers.¹² Anthracene derivatives were coupled with the **g**-unit, and their assembling behaviour and optical properties were evaluated.

Experimental

Materials: 9-bromo anthracene, 4-carboxyphenylboronic acid, palladium diacetate, 9-(*p*-carboxyphenyl)anthracene, 9-phenyl,10-bromo anthracene, tetrakis(triphenylphosphine), and boron tribromide were purchased from Tokyo Chemical Industry. N^1,N^5 -didodecyl-L-glutamide and lipid (**g**) and N -bromo- N^1,N^5 -didodecyl-L-glutamide were synthesized by the previously reported procedure.

^a Department of Applied Chemistry & Biochemistry, Kumamoto University, Kumamoto 860-8555, Japan

^b Université de Bordeaux, CNRS, Institut des Sciences Moléculaires - UMR 5255, NEO Nanostructures Organiques, 33400 Talence, France

^c Kumamoto Institute for Photo-Electro Organics (PHOENICS), Kumamoto, 862-0901, Japan

† Footnotes relating to the title and/or authors should appear here.

Electronic Supplementary Information (ESI) available: Fluorescence quantum yield and gelation properties of anthracene derivatives, CD, UV-vis and fluorescence spectra and TEM images. See DOI: 10.1039/x0xx00000x

Instrumentation: UV-visible, CD, fluorescence and CPL spectra were measured with V-560 (JASCO), J725 (JASCO), FP-6500 (JASCO), and CPL200 (JASCO), respectively. TEM images were observed with JEM-2100 (JEOL). ¹H NMR (400 MHz) spectra were recorded in CDCl₃, SiMe₄ as an internal standard with JNM-EX400 (JEOL). IR spectra were measured in a KBr method with FT/IR-4100 (JASCO).

Synthesis: Three anthracene derivatives (**g-PA**, **g-PA-2**, and **g-DPA**) were synthesized following procedures.

***N,N'*-Didodecyl-L-glutamide-9-(phenoxyacetic acid)anthracene (**g-PA**):**

9-(Phenoxyacetic acid)anthracene (50 mg, 0.15 mmol) and *N,N'*-didodecyl-L-glutamide (90 mg, 0.19 mmol) were dissolved in CH₂Cl₂ (30 mL) in the presence of triethylamine (0.12 mL, 0.8 mmol) and diethyl cyanophosphate (0.15 mL, 0.8 mmol) at 0 °C. The mixture solution was stirred at room temperature for 6 h. The solution was washed three times with 0.2 N-NaOH aq., 0.2-N HCl, and distilled water. After drying by Na₂SO₄, CH₂Cl₂ was removed under reduced pressure and the residue was purified by recrystallization (methanol) to give **g-PA** as a white yellow powder (73.9 mg, 62%). mp 149-151 °C, FT-IR (KBr): 3277(ν_{N-H}), 3083 (ν_{Ar-H}), 2923, 2851(ν_{C-H}), 1669, 1641 ($\nu_{C=O(amide)}$), 1552 (δ_{N-H}). ¹H NMR (400 MHz; CDCl₃; Me₄Si): 0.86-0.89 (6H, t, *J* = 6.8 Hz, -CH₃), 1.23-1.25 (36H, br, -(CH₂)₉-), 1.51-1.53 (4H, br, NH-CH₂-CH₂-), 2.07-2.18 (2H, m, -C*HCH₂-), 2.35-2.45 (2H, m, -CH₂CO-), 3.28 (4H, br, -NHCH₂-), 4.51-4.52 (1H, m, -C*H-), 4.62-4.65 (2H, s, -OCH₂-), 5.92 (1H, s, NH), 6.83 (1H, s, NH), 7.18-7.20 (2H, m, ArH), 7.33-7.39 (4H, m, ArH), 7.44-7.47 (2H, m, ArH), 7.65-7.67 (2H, m, ArH), 8.03-8.05 (2H, m, ArH), 8.49 (1H, s, ArH). Elemental analysis calcd for C₅₁H₇₃N₄O₃: C, 77.33; H, 9.29; N, 5.30. Found: C, 76.98; H, 8.87; N, 5.28%.

9-(*p*-carboxyphenyl)anthracene: 9-Bromo anthracene (676 mg, 2.67 mmol) and 4-carboxyphenylboronic acid (443 mg, 3.20 mmol) were dissolved in dry DMF (30 mL). The mixed solution was bubbled by N₂ gas for 30 min. Palladium diacetate (50 mg) was added to the mixed solution and stirred for 30 min. A potassium carbonate aqueous solution (30 mL, 3.75 mmol) was added slowly and stirred at 130 °C for 24 hours and the conversion was monitored via TLC (hydrophobic silica, ethanol/chloroform 9:1 v/v, R_f = 0.8). The reacted solution was filtrated by glass filter with Celite. The filtrated solution was washed three times with distilled water and 0.1 N NaOH aq. The obtained aqueous solution was acidified with 1 N HCl aq. to pH 2.0. The precipitates were filtered and dried *in vacuo*, to give 9-(*p*-carboxyphenyl)anthracene (300 mg, 38%) as a white powder. mp 260-261 °C. ν_{max} (KBr)/cm⁻¹ 2977 ($\nu_{C=O(OH)}$), 1686 ($\nu_{C=O(OH)}$). δ_H (400 MHz, CDCl₃, Me₄Si) 7.25-8.55 (m, 13H, ArH). Elemental analysis calcd for C₂₁H₁₄O₂: C, 84.5; H, 4.7. Found: C, 83.2; H, 4.5%.

***N,N'*-Didodecyl-L-glutamide-9-(*p*-carboxyphenyl)**

phenylanthracene (g-PA-2**):** 9-(*p*-carboxyphenyl)anthracene (200 mg, 0.67 mmol) and *N,N'*-didodecyl-L-glutamide (269 mg, 0.56 mmol) were dissolved in dry THF (20 mL) in the presence of triethylamine (0.23 mL, 1.68 mmol) and diethyl cyanophosphate (0.21 mL, 1.34 mmol) at 0 °C. The mixture

solution was stirred at 25 °C for 24 h and the conversion was monitored via TLC (hydrophobic silica, ethanol/chloroform 9:1 v/v, R_f = 0.6). The reacted solution was evaporated for removing THF. The obtained residue was dissolved in chloroform and washed three times with 0.2 N-HCl, 0.2 N-sodium hydrogen carbonate aq. and distilled water. After dried by Na₂SO₄, chloroform was removed under reduced pressure and the residue was purified by recrystallization (methanol) to give **g-PA-2** as a white powder (189 mg, 43%). mp 157.6-163.0 °C. ν_{max} (KBr)/cm⁻¹ 3292 (ν_{N-H}), 2919(ν_{C-H}), 2849(ν_{C-H}), 1628 (ν_{amide}), 1534(δ_{NH}). δ_H (400 MHz, CDCl₃, Me₄Si) 0.85-0.88(m, 6H, CH₃), 1.22-1.25(m, 36H, (CH₂)₉), 1.59 (m, 4H, NHCH₂CH₂), 2.11-2.24 (q, 2H, C*HCH₂), 2.33-2.49 (q, 2H, C*HCH₂), 3.27-3.31 (m, 4H, NHCH₂), 4.60-4.70 (q, 1H, C*H), 6.01-6.10 (br, 1H, NH), 6.95-7.05 (m, 1H, NH), 7.25-8.52 (m, 13H, ArH). Elemental analysis calcd for C₅₀H₇₁N₃O₃: C, 78.8; H, 9.4, N, 5.5. Found: C, 78.7; H, 9.4; N, 5.3%.

9-(*p*-methoxyphenyl),10-phenylanthracene (DPA-OCH₃**):** 9-Phenyl,10-bromo anthracene (700 mg, 2.10 mmol) and 4-carboxyphenylboronic acid (402 mg, 2.83 mmol) were dissolved in dry toluene (35 mL). The mixed solution was bubbled by N₂ gas for 30 min. Tetrakis(triphenylphosphine) (50 mg) was added to the mixed solution and stirred for 30 min. A potassium carbonate aqueous solution (30 mL, 3.75 mmol) was added slowly and stirred at 90 °C for 24 hours and the conversion was monitored via HPLC (ODS column 250 mm × 4.5 mm, mobile phase: methanol, detection: UV (420 nm)). A sodium carbonate (20%) aq./*n*-hexane (2 : 3) mixture was added to the reacted solution and precipitates were filtrated. The obtained powder was purified by recrystallization (*n*-hexane) to give **DPA-OCH₃** as a gray powder (296 mg, 39%). mp 247.1-250.0 °C. ν_{max} (KBr)/cm⁻¹ 3063 ($\nu_{C=C}$), 1244(ν_{O-C}). δ_H (400 MHz, CDCl₃, Me₄Si) 3.96(m, 3H, OCH₃), 7.12-7.75 (m, 15H, ArH). Elemental analysis calcd for C₂₇H₂₀O: C, 89.9; H, 5.6. Found: C, 89.1; H, 5.6%.

9-(*p*-Hydroxyphenyl),10-phenylanthracene (DPA-OH**):** Boron tribromide (17% in CH₂Cl₂) (1.4 mL, 1.4 mmol) was added to **DPA-OCH₃** (250 mg, 0.69 mmol) dissolved CH₂Cl₂ solution, and stirred at 25 °C for 24 h and the conversion was monitored via TLC (silica, *n*-hexane/ CH₂Cl₂ 1:6 v/v, R_f = 0.3). The reacted solution was washed three times with 0.2 N-HCl and saturated saline. After dried by Na₂SO₄, CH₂Cl₂ was removed under reduced pressure and the residue was purified by recrystallization (ethanol) to give **DPA-OH** as a yellow powder (150 mg, 78%). mp 277.0-279.8 °C. ν_{max} (KBr)/cm⁻¹ 3428 (ν_{O-H}), 3062 ($\nu_{C=C}$). δ_H (400 MHz, CDCl₃, Me₄Si) 4.82-5.11 (m, 1H, OH), 7.02-7.79 (m, 15H, ArH). Elemental analysis calcd for C₂₆H₁₈O: C, 90.1; H, 5.2. Found: C, 88.3; H, 5.4%.

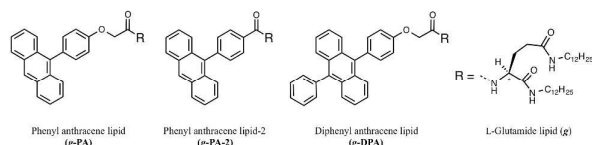
***N,N'*-Didodecyl-L-glutamide-9-(phenoxyacetic acid),10-phenylanthracene (**g-DPA**):** **DPA-OH** (110 mg, 0.32 mmol), *N*-bromo-*N'*,*N'*-didodecyl-L-glutamide (185 mg, 0.3 mmol), and potassium carbonate (54 mg, 0.39 mmol) were dissolved in 2-butanone (40 mL). The mixture was stirred at 80 °C for 24 h and the conversion was monitored via TLC (silica, CH₂Cl₂, R_f = 0.8). The reacted solution was washed three times with 0.2 N-HCl, 0.2 N-sodium hydrogen carbonate aq. and distilled water. After dried by Na₂SO₄, 2-butanone was removed under

reduced pressure and the residue was purified by recrystallization (methanol) to give **g-DPA** as a yellow powder (72.2 mg, 27%). mp 167.2-170.0 °C. $\nu_{\max}(\text{KBr})/\text{cm}^{-1}$ 3291 ($\nu_{\text{N-H}}$), 2957 ($\nu_{\text{C-H}}$), 2851 ($\nu_{\text{C-H}}$), 1624 (ν_{amide}), 1553 (δ_{NH}). δ_{H} (400 MHz, CDCl_3 , Me_4Si) 0.85-0.89 (m, 6H, CH_3), 1.18-1.24 (m, 36H, $(\text{CH}_2)_9$), 1.52 (m, 4H, NHCH_2CH_2), 2.01-2.22 (q, 2H, C^*HCH_2), 2.31-2.51 (q, 2H, C^*HCH_2), 3.32-3.49 (m, 4H, NHCH_2), 4.62-4.64 (q, 1H, C^*H), 4.72 (m, 2H, $\text{O-CH}_2\text{-C=O}$), 5.95-5.98 (br, 1H, NH), 6.86-6.93 (br, 1H, NH), 7.21-8.13 (m, 15H, ArH). Elemental analysis calcd for $\text{C}_{57}\text{H}_{77}\text{N}_3\text{O}_4$: C, 78.9; H, 8.9; N, 4.8, Found: C, 77.8; H, 9.0; N, 4.6%.

Preparation of g-PA-incorporated LDPE and PVB film: The **g-PA** powder was mixed into low-density polyethylene (LDPE) powder or polyvinyl butyral (PVB), and heated at 150 °C using hot pressing machine (MNP-001, AS ONE). The mixture was heated at 120 °C and pressed three times. After cooling, the **g-PA**-incorporated LDPE and PVB film (0.5 wt%) were obtained with 500 μm thickness.

Calculation of the CPL dissymmetry factor g_{lum} : The CPL dissymmetry factor g_{lum} was obtained as $2(I_L - I_R)/(I_L + I_R)$ at the wavelength of the CPL intensity maximum (540 nm). I_L and I_R are left and right circularly polarized light, respectively.

Results and discussion



Scheme 1. Chemical structures of L-glutamide functionalized phenyl anthracene (**g-PA** and **g-PA-2**) and diphenyl anthracene (**g-DPA**).

Three types of anthracene lipids, [9-(phenoxyacetic acid)anthracene lipid (**g-PA**), 9-(*p*-carboxyphenyl)anthracene lipid (**g-PA-2**), and 9-(phenoxyacetic acid),10-phenylanthracene lipid (**g-DPA**)], were synthesized by above procedure (Scheme 1). These anthracene lipids are soluble in various organic solvents such as methanol, ethanol, tetrahydrofuran (THF), chloroform and toluene. Optical properties such as the absorption maxima and the fluorescence quantum yield are summarized in Table S1. The anthracene lipids have absorption bands in the UV region and emitted light in the deep blue region of the spectrum at around 420 nm in solution with high quantum yields (Fig. S1). In the solid state, the fluorescence wavelength shifted towards longer wavelengths, and the fluorescence quantum yields decreased to moderate or low values due to the formation of an excimeric state of anthracene moieties. When the solvent was changed to a poor solvent such as cyclohexane or *n*-hexane, the anthracene lipid solutions made a gel (Table S2). As shown in Fig. S2, all anthracene gels showed red-shifted absorption bands with a negative Cotton effect. These spectral changes indicate that the anthracene moieties formed a *J*-type

(slipped face-to-face) and *S*-chiral (left-handed twist) orientation in the gel state. As shown in fluorescence spectra of anthracene in the gel state, the emission shifted to longer wavelengths compared to solution. In particular, the **g-PA** gel prepared from an *n*-hexane/THF (50:1) mixed solution showed a drastic emission shift. Although the absorption maximum of **g-PA** shifted by only 5 nm (383 nm to 388 nm), the fluorescence maximum shifted 100 nm (426 nm to 526 nm) when changing from solution to gel. These spectral changes were caused by an excimer formation of the anthracene fluorophore. It has been reported that anthracene forms three types of excimers with a slightly different stacking formation in the excited state.¹³ The first is a partially-overlapped formation (overlapping at an angle of 55°) with a fluorescence maximum near 470 nm (**E1**). The second is a T-shaped excimer with a fluorescence maximum near 510 nm (**E2**). The last is a sandwich type excimer because anthracene units are symmetrically π -stacked with a fluorescence maximum near 560 nm (**E3**). Based on this knowledge, the three anthracene derivatives were classified as follows. The **g-PA** assembly has **E1** and **E3** states, the **g-PA-2** assembly has **E1** and monomeric states, and the **g-DPA** assembly has a large amount of monomeric state with little amount of **E1** state. The reason that the **g-DPA** could not form excimer formation was explained by molecular structure. The steric hindrance of diphenyl moiety of **g-DPA** inhibited the π -stacking of anthracene.

Based on the above results, we focused on the self-assembly of **g-PA**. The transmission electron microscope (TEM) images of **g-PA** assemblies in a film prepared from an *n*-hexane/THF (50:1) mixed gel showed well-developed fibrous networks (Fig. S3). The optical properties of **g-PA** can be controlled by changing the concentration, changing the solvent or changing the temperature. The absorption and fluorescence bands shifted to shorter wavelengths and a decrease in the circular dichroism (CD) signal was observed when the concentration of **g-PA** was decreased or the THF ratio was increased (Fig. S4 and S5). This indicates that the **g-PA** transformed from the gel (oriented) state to the solution (dispersed) state by changing the concentration and solvent.

The spectral change of **g-PA** with temperature showed interesting phenomena. When the temperature was increased from 10 °C to 60 °C, the absorption and fluorescence bands shifted to shorter wavelengths (Fig. 1). However, the **g-PA** solution still kept the physical gel state with negative CD signal at 60 °C (Fig. 1c). Also, the **g-PA** gel exhibited different fluorescence spectra when the cooling process was changed. As shown in Fig. 2a, the **g-PA** gel prepared by slow cooling from 60 °C to 10 °C via keeping for 30 min at 35 °C emitted green fluorescence and the excimer formation ratio, which is the fluorescence intensity of the excimer at 526 nm *versus* that of the monomer at 426 nm (I_{526}/I_{426}), was higher ($I_{526}/I_{426} = 2.3$) than that of the **g-PA** gel that was prepared by rapid cooling from 60 °C to 10 °C ($I_{526}/I_{426} = 1.2$).

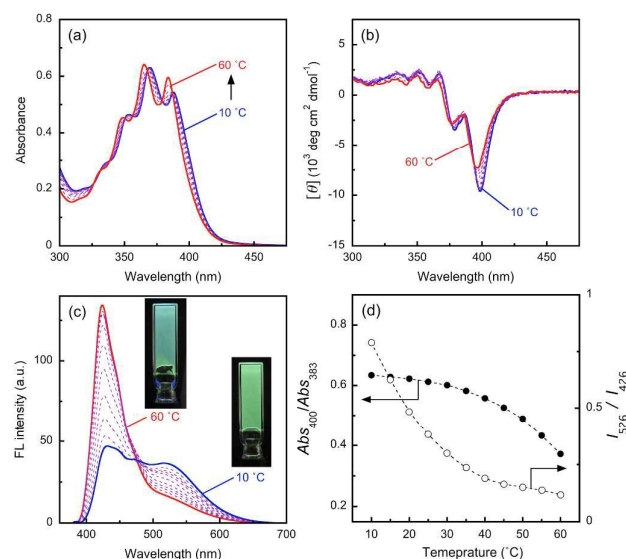


Figure 1. Temperature-dependent (a) UV-vis, (b) CD and (c) fluorescence spectra of **g-PA** (2 mM) in *n*-hexane/THF (50:1). The excitation wavelength was 385 nm. The arrow indicates a temperature increase from 10 °C to 60 °C. The inset shows photo image of **g-PA** gel (2 mM) in *n*-hexane/THF (50:1) under UV (365 nm) light. (d) Change in the temperature-dependent absorbance ratio (solid circles) and fluorescence intensity ratio (open circles).

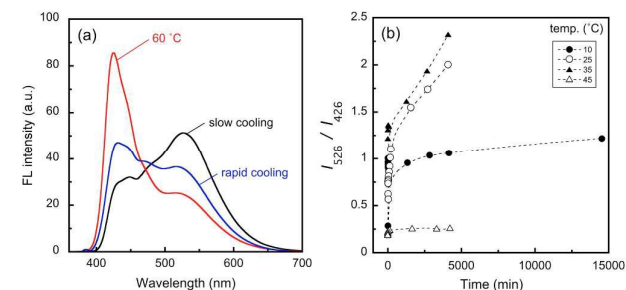


Figure 2. (a) Fluorescence spectra of **g-PA** (2 mM) in an *n*-hexane/THF (50:1) mixture. The red line was measured at 60 °C and the blue line is the spectrum from the gel that was prepared by rapid cooling process from 60 °C to 10 °C. The black line is the spectrum from a gel that was prepared by slow cooling process from 60 °C to 10 °C via 35 °C. (b) Time-dependent fluorescence intensity ratio changes of **g-PA** (2 mM) in an *n*-hexane/THF (50:1) mixture at various temperatures.

To determine the nature of the temperature dependence, the spectral changes were monitored as a function of time at various temperatures (Fig. 2b, Fig. S6). For this measurement, the **g-PA** solution was heated at 60 °C for 30 min and then was kept at a constant temperature (10, 25, 35 or 45 °C). The excimer emission at 526 nm increased with time, and the excimer formation ratio (I_{526}/I_{426}) of the **g-PA** gel increased from 0.2 to ~ 2.0 by keeping the solution at 25 or 35 °C for 4000 min. Similar spectral changes were not observed at 10 and 45 °C. The I_{526}/I_{426} reached only 1.2 when the **g-PA** solution was kept at 10 °C for 14000 min. The excimer emission at 526 nm did not increase and the I_{526}/I_{426} reached 0.3 when the solution was kept at 45 °C for 4200 min.

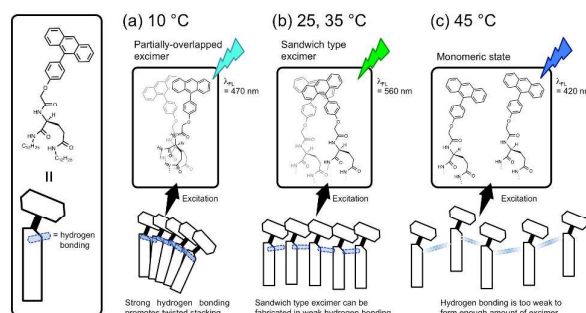


Figure 3. Schematics of the assembly and excimer formation of **g-PA** in an *n*-hexane/THF (50:1) mixture at (a) 10 °C, (b) 25 and 35 °C, and (c) 45 °C.

There was no clear difference in the UV-vis spectra with temperature (10, 25, 35 and 45 °C). The rate of change in the absorbance, which is the absorbance of *J*-type ordered anthracene at 400 nm versus that of disordered anthracene at 383 nm (Abs_{400}/Abs_{383}), reached ~ 0.6 by keeping the solution at 10, 25 and 35 °C for >5000 min (Fig. S7).

Based on these results, we determined that **g-PA** forms three types of assemblies. At high temperatures (for example, 45 °C), **g-PA** is not well-ordered and there is a large amount of monomeric state and a small amount of sandwich-type excimeric state of the anthracene fluorophore (**E3**). At medium temperatures (25 and 35 °C), **g-PA** forms a macroscopic gel and can also form well ordered stacks of anthracene fluorophores. Almost all anthracene fluorophores exist as excimers [partially-overlapped excimer (**E1**) and (**E3**)]. At a low temperature (10 °C), **g-PA** immediately forms a macroscopic gel. However, the composition of the excimer is different from that of the **g-PA** gel formed at medium temperatures. The amount of **E1** is larger and that of **E3** is smaller. These differences are similar to that previously reported.^{11, 14} At low temperatures, intermolecular hydrogen bonding through the amide bonds located around the chiral carbon became strong and promoted the twisted stacking of the anthracene fluorophore. The formation of the twisted stacks induced the partially overlapped excimer of anthracene (**E1**) as shown in Fig. 3a. At medium temperatures, intermolecular hydrogen bonding is weaker than at low temperatures. Therefore, the anthracene fluorophores can move to change the stacking to an **E3**-type excimer in the excited state (Fig. 3b). At high temperatures, intermolecular hydrogen bonding became weak, therefore most anthracene fluorophores could not form an excimer (Fig. 3c). The precise control of the fluorescence wavelength was accomplished by changing the temperature, solvent and the cooling process.

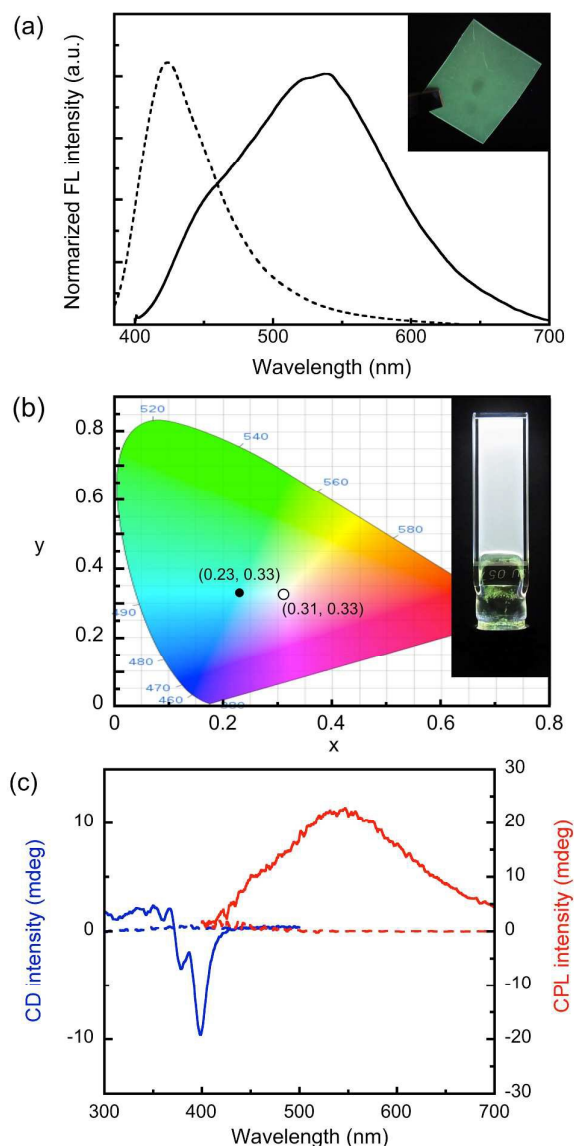


Figure 4. (a) Fluorescence spectra of 0.5 wt% **g-PA** incorporated into an LDPE film (solid line) and PVB film (dotted line). The inset is a photograph of the **g-PA** incorporated LDPE film under UV light (365 nm). (b) CIE 1931 chromaticity coordinates of the **g-PA** (2 mM) gel at 35 °C (solid circle) and the **g-PA** (2 mM) with **NR** (0.03 mM) gel (open circle) in an *n*-hexane/THF (50:1) mixture at 25 °C. The inset is a photograph of the **g-PA/NR** gel under UV light (365 nm). (c) CD (blue line) and CPL (red line) spectra of the **g-PA** (2 mM) gel in an *n*-hexane/THF (50:1) mixture (solid line) and in THF (dotted line) at 25 °C. The excitation wavelength was 330 nm.

The highly oriented **g-PA** assemblies had three interesting characteristics that are important for future applications such as a spectral conversion polymer film, in white-light emitting diodes, and in circular polarized displays. The first is efficient excimer emission in the solid polymer film. **g-PA** was incorporated into a low-density polyethylene (LDPE) film and polyvinyl butyral (PVB) film prepared by a hot-pressing method. The **g-PA**-incorporated LDPE film showed green fluorescence at 537 nm, which means that it was an **E3**-type excimer of anthracene (Fig. 4a). Alternatively, the **g-PA**-

incorporated PVB film emitted blue fluorescence at 422 nm, which means that it was a monomer of anthracene. The similar monomeric emission was observed by using phenyl anthracene instead of **g-PA**, or decreasing the concentration of **g-PA** (Fig. S8). This indicates that **g-PA** forms highly oriented assemblies, and that the fluorescence wavelength can be controlled not only in solution but also in the solid polymer film. The second is white-light fluorescence. A 2mM **g-PA** gel showed greenish white-light fluorescence at 35 °C. The Commission International de l'Eclairage (CIE) colour coordinates of the **g-PA** gel were (0.23, 0.33). By adding a small amount (0.03 mM) of 9-diethylamino-5-benzo[α]phenoxazinone [Nile red (**NR**)], the **g-PA** gel (2 mM, *n*-hexane:THF = 50:1) emitted white light at 25 °C with CIE coordinates of (0.31, 0.33) when excited at 385 nm. This is close to those of pure white light, (0.33, 0.33) (Fig. 4b). A mixture of **g-PA** (2 mM) with **NR** (0.03 mM) in THF did not emit white light but emitted a purple/red colour with CIE coordinates of (0.19, 0.04) at 25 °C (Fig. S9). This indicates that the white-light fluorescence was accomplished through not only the addition of **NR** but also the supramolecular gelation. The third is circular polarized luminescence (CPL). The **g-PA** (2 mM) gel emitted clear CPL at 540 nm assigned to the **E3**-type excimer, with a dissymmetry factor, of 3.2×10^{-3} in a mixture of *n*-hexane/THF (50:1) at 25 °C (Fig. 4c). Similar CPL was not detected using THF instead of an *n*-hexane/THF (50:1) mixture as solvent. This result indicates that the CPL was generated through the supramolecular gelation.

Conclusions

We fabricated a highly ordered anthracene assembly that had a widely colour-tunable fluorescence emission wavelength and polarization through supramolecular gelation. This anthracene assembly had various stacking formations depending on the local environment, which could be controlled by the temperature, solvent and concentration. In addition, these results were able to be reproduced in solid polymer films. White light emission was achieved through the addition of a small amount of NR dye. We believe that this colour-tunable material could have applications in displays, OLEDs, spectral conversion films and sensors.

Acknowledgements

This work was supported by a Grant-in-Aid for Young Scientists (B) (No. 25810119) and for Program for Regional Innovation Strategy Support Program from the Ministry of Education, Culture, Sports, Science and Technology of Japan.

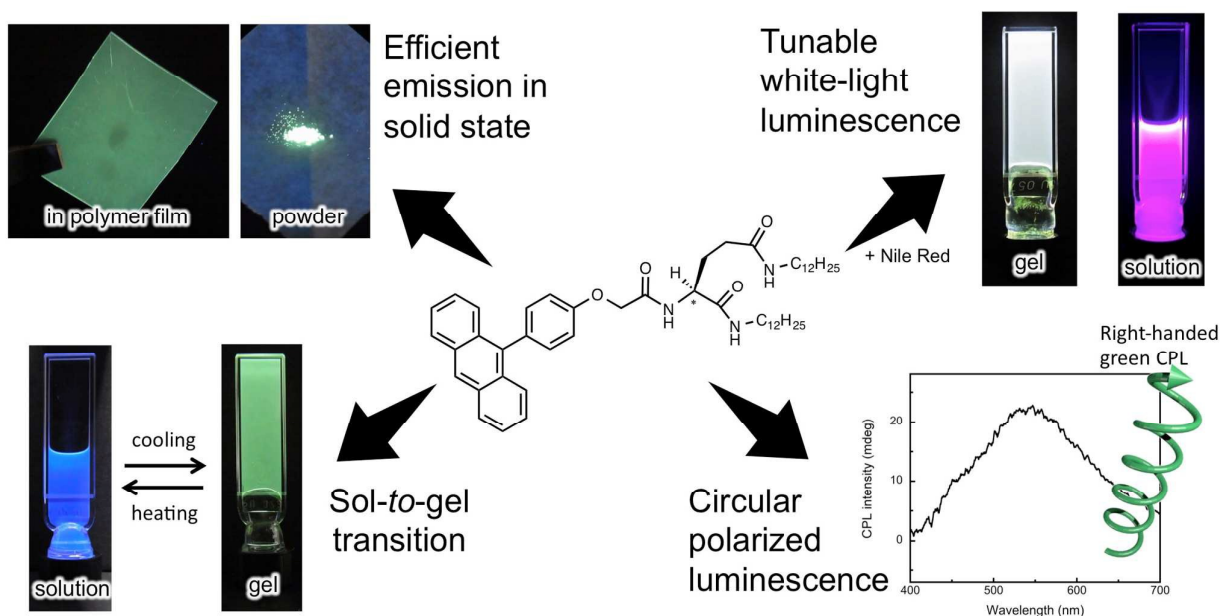
Notes and references

- (a) Q. Zhang, B. Li, S. Huang, H. Nomura, H. Tanaka and C. Adachi, *Nat. Photo.*, 2014, **8**, 326; (b) C. M. Tyrakowski and P. T. Snee, *Anal. Chem.*, 2014, **86**, 2380; (c) L. Shi, Y. Fu, C. He, D. Zhu, Y. Gao, Y. Wang, Q. He, H. Cao and J. Cheng, *Chem.*

- Commun.*, 2014, **50**, 872; (d) B. A. San Jose, J. Yan and K. Akagi, *Angew. Chem. Int. Ed. Engl.*, 2014, **53**, 10641; (e) B. Gole, A. K. Bar and P. S. Mukherjee, *Chem. Eur. J.*, 2014, **20**, 2276; (f) H. Uoyama, K. Goushi, K. Shizu, H. Nomura and C. Adachi, *Nature*, 2012, **492**, 234.
- 2 (a) E. Benedetti, L. S. Kocsis and K. M. Brummond, *J. Am. Chem. Soc.*, 2012, **134**, 12418; (b) X. Ma, Y. Wang, T. Zhao, Y. Li, L. C. Su, Z. Wang, G. Huang, B. D. Sumer and J. Gao, *J. Am. Chem. Soc.*, 2014, **136**, 11085.
- 3 (a) Q. Gong, Z. Hu, B. J. Deibert, T. J. Emge, S. J. Teat, D. Banerjee, B. Mussman, N. D. Rudd and J. Li, *J. Am. Chem. Soc.*, 2014, **136**, 16724; (b) V. Jankus, P. Data, D. Graves, C. McGuinness, J. Santos, M. R. Bryce, F. B. Dias and A. P. Monkman, *Adv. Funct. Mater.*, 2014, **24**, 6178; (c) Y. K. Jung, M. A. Woo, H. T. Soh and H. G. Park, *Chem Commun*, 2014, **50**, 12329; (d) X. Zhang, W. Liu, G. Z. Wei, D. Banerjee, Z. Hu and J. Li, *J. Am. Chem. Soc.*, 2014, **136**, 14230.
- 4 (a) H. Shono, T. Ohkawa, H. Tomoda, T. Mutai and K. Araki, *ACS Appl. Mater. Interfaces*, 2011, **3**, 654; (b) T. Mutai, H. Tomoda, T. Ohkawa, Y. Yabe and K. Araki, *Angew. Chem. Int. Ed. Engl.*, 2008, **47**, 9522; (c) P. Xue, B. Yao, J. Sun, Z. Zhang and R. Lu, *Chem. Commun.*, 2014, **50**, 10284; (d) W. Weigel and W. Rettig, *J. Phys. Chem A*, 2003, **107**, 5941; (e) X. He, J. Borau-Garcia, A. Y. Woo, S. Trudel and T. Baumgartner, *J. Am. Chem. Soc.*, 2013, **135**, 1137; (f) X. Yang, R. Lu, P. Xue, B. Li, D. Xu, T. Xu and Y. Zhao, *Langmuir*, 2008, **24**; (g) J. D. Cheon, T. Mutai and K. Araki, *Org. Biomol. Chem.*, 2007, **5**, 2762.
- 5 (a) H. Hayasaka, T. Miyashita, K. Tamura and K. Akagi, *Adv. Funct. Mater.*, 2010, **20**, 1243; (b) C. Vijayakumar, V. K. Praveen and A. Ajayaghosh, *Adv. Mater.*, 2009, **21**, 2059; (c) K. Watanabe, I. Osaka, S. Yorozyua and K. Akagi, *Chem. Mater.*, 2012, **24**, 1011.
- 6 (a) F. B. Dias, K. N. Bourdakos, V. Jankus, K. C. Moss, K. T. Kamtekar, V. Bhalla, J. Santos, M. R. Bryce and A. P. Monkman, *Adv. Mater.*, 2013, **25**, 3707; (b) C. C. Hsieh, P. T. Chou, C. W. Shih, W. T. Chuang, M. W. Chung, J. Lee and T. Joo, *J. Am. Chem. Soc.*, 2011, **133**, 2932; (c) Y. Ren, W. H. Kan, M. A. Henderson, P. G. Bomben, C. P. Berlinguette, V. Thangadurai and T. Baumgartner, *J. Am. Chem. Soc.*, 2011, **133**, 17014; (d) S. R. Grando, C. M. Pessoa, M. R. Gallas, T. M. Costa, F. S. Rodembusch and E. V. Benvenuto, *Langmuir*, 2009, **25**, 13219.
- 7 (a) A. G. L. Olive, A. D. Guerzo, C. Schafer, C. Belin, G. Raffy and C. Giansante, *J. Phys. Chem C*, 2010, **114**, 10410; (b) T. Ikeda, T. Masuda, T. Hirao, J. Yuasa, H. Tsumatori, T. Kawai and T. Haino, *Chem. Commun.*, 2012, **48**, 6025; (c) S. S. Babu, V. K. Praveen and A. Ajayaghosh, *Chem. Rev.*, 2014, **114**, 1973.
- 8 (a) K. Kondo, A. Suzuki, M. Akita and M. Yoshizawa, *Angew. Chem. Int. Ed. Engl.*, 2013, **52**, 2308; (b) Y. Sagara and T. Kato, *Angew. Chem. Int. Ed.*, 2008, **47**, 5175; (c) A. Dawn, T. Shiraki, S. Haraguchi, H. Sato, K. Sada and S. Shinkai, *Chem. Eur. J.*, 2010, **16**, 3676; (d) I. O. Shklyarevskiy, P. Jonkheijm, P. C. M. Christianen, A. P. H. J. Schenning, A. D. Guerzo, J.-P. Desvergne, E. W. Meijer and J. C. Maan, *Langmuir*, 2005, **21**, 2108; (e) J.-P. Desvergne, F. Fages, H. Bouas-Laurent and P. Marsau, *Pure Appl. Chem.*, 1992, **64**, 1231.
- 9 (a) M. Takafuji, A. Ishiodori, T. Yamada, T. Sakurai and H. Ihara, *Chem. Commun.*, 2004, 1122; (b) Y. Li and M. Liu, *Chem. Commun.*, 2008, 5571; (c) X. Yang, G. Zhang, D. Zhang and D. Zhu, *Langmuir*, 2010, **26**, 11720; (d) W. Miao, L. Zhang, X. Wang, H. Cao, Q. Jin and M. Liu, *Chem. Eur. J.*, 2013, **19**, 3029.
- 10 (a) H. Jintoku and H. Ihara, *Chem. Commun.*, 2012, **48**, 1144; (b) H. Jintoku, T. Sagawa, M. Takafuji and H. Ihara, *Chem. Eur. J.*, 2011, **17**, 11628; (c) H. Jintoku, T. Sagawa, K. Miyamoto, M. Takafuji and H. Ihara, *Chem. Commun.*, 2010, **46**, 7208; (d) H. Jintoku, T. Sagawa, M. Takafuji and H. Ihara, *Org. Biomol. Chem.*, 2009, **7**, 2430.
- 11 H. Jintoku, Y. Okazaki, M. Takafuji and H. Ihara, *Chem. Lett.*, 2013, **42**, 1297.
- 12 (a) G. C. Balazs, A. del Guerzo and R. H. Schmehl, *Photochem Photobiol Sci*, 2005, **4**, 89; (b) A. Dawn, N. Fujita, S. Haraguchi, K. Sada and S. Shinkai, *Chem. Commun.*, 2009, 2100; (c) Y. Kikkawa, H. Kihara, M. Takahashi, M. Kanetsato, T. S. Balaban and J.-M. Lehn, *J. Phys. Chem. B*, 2010, **114**, 16718.
- 13 (a) P. K. Lekha and E. Prasad, *Chem. Eur. J.*, 2010, **16**, 3699; (b) M. Jaseer and E. Prasad, *J. Photochem. Photobiol., A*, 2010, **214**, 248; (c) G. Zhang, G. Yang, S. Wang, Q. Chen and J. S. Ma, *Chem. Eur. J.*, 2007, **13**, 3630.
- 14 H. Jintoku, M. Yamaguchi, M. Takafuji and H. Ihara, *Adv. Funct. Mater.*, 2014, **24**, 4105.

Tunable Stokes Shift and Circular Polarized Luminescence by Supramolecular Gel

Hirokuni Jintoku, Min-Tzu Kao, André Del Guerso, Yudai Yoshigashima, Takuya Masunaga, Makoto Takafuji and Hirotaka Ihara



A new optical material based on the self-assembly of a low-molecular organogelator for the control of the fluorescence wavelength and polarization was developed.